CLM-P737

UKAEA

Preprint

CHARGE EXCHANGE OBSERVATIONS AND ANALYSIS IN THE DITE TOKAMAK

B. P. DUVAL
N. C. HAWKES
S. J. FIELDING
R. C. ISLER
N. J. PEACOCK

CULHAM LABORATORY
Abingdon Oxfordshire
1985

CLM-P 737

CHARGE EXCHANGE OBSERVATIONS AND ANALYSIS IN THE DITE TOKAMAK

B P Duval*, N C Hawkes, S J Fielding, R C Isler+ and N J Peacock

Culham Laboratory, Abingdon, Oxon, OX14 3DB
(EURATOM/UKAEA Fusion Association)

* Clarendon Laboratory, Oxford University
\+ ORNL, Oak Ridge, Tennessee, USA

ABSTRACT

Measurements of the enhancement of line intensities from Oxygen and Carbon ions during beam injection of hydrogen atoms into the DITE Tokamak have been made for neutral energies of 25keV and beam powers up to 2 MW. Observations of the spectrum from O encompass the Lyman series in the XUV region (1s-np, $n < 9$) and $\Delta n=1$ transitions in the VUV and visible regions. The different selection rules for these transitions allow a differentiation between C/X and electron impact excitation of the different (n, l) states. Using theoretical cross-sections and a cascade model for C/X recombination in to hydrogenic ions, the concentrations of impurity nuclei (eg: O^{8+}) are determined from the $\Delta n=1$ VUV lines. This analysis is unsuitable for the Lyman series which lack the C/X signature. Their intensity is determined primarily by the ionisation balance, and excitation from the ground state hydrogenic ion. l state mixing is considered. No indication of statistical repopulation of the sublevels is observed for $n < 7$.

(Submitted for publication in J. Nucl. Instr. and Methods)

February 1985

1. INTRODUCTION

In the Tokamak plasma, one approach to raising the plasma energy content is to use high energy neutral beams which cross the magnetic field lines and deposit their kinetic energy into the plasma. Following earlier work on the expected ionisation balance changes (Clark et al (1982)) resulting from neutral beam injection into the DITE Tokamak, direct Charge-Exchange (C/X) radiation from impurity ions has now been studied. Charge exchange of these neutrals with ions already in the plasma can have a significant cross section, especially for the fully or partially stripped impurities always present in Tokamak devices. Low-Z impurities eg: O and C at the typical electron temperature of 700 eV present in DITE exist in a fully stripped state in the core and over most of the plasma radius.

The typical C/X reaction:

eg: $$O^{8+} + H^0 \rightarrow O^{(7+)*} + H^+$$

leaves the recombined ion in an excited state. Spectroscopic observation of the decay of these ions, yields information on the spatial distribution of the fully stripped impurities and in addition, may serve as a diagnostic of the beam absorption. Before injection the line intensities associated with transitions between exited states not connected to the ground state are normally low relative to the resonance lines from the same upper level. Therefore any instantaneous intensity change following beam injection may be ascribed solely to the C/X process. Also for fully stripped ions, the collision involves only three particles and tends to be the simplest to treat theoretically. Since C/X radiation is only observed from the region where the neutral beam intersects the spectrometer acceptance cone, then by scanning the intersection over the plasma volume with a probe beam, (Fonck, Finkenthal et al (1982)), spatially localised measurements may be made. C/X emission has been used to determine plasma parameters such as impurity density as in this paper, (Fonck et al (1982), Isler et al (1981)), ion temperature, (Fonck et al (1983), Groebner et al (1983)), and bulk plasma rotation, (Hawkes and Peacock (1985), Isler and Murray (1983)). Spatially resolved measurements are possible as in the experiments on the neutral beam profiles, Skinner et al (1984).

2. EXPERIMENTAL APPARATUS

Results are given only for Oxygen, although in the UV and visible

regions data from Carbon (the DITE limiter material) has also been obtained. The instrument locations round the machine are shown in Fig 1. In the XUV region, for the n=2-1, 3-2 and 4-3 transitions, a 2m absolutely calibrated, grazing incidence instrument was used with a slitted, channeltron detector, while the longer wavelength 5-4 and 6-5 transitions were measured using a 1m normal incidence spectrometer equipped with a reticon diode detector preamplified by a microchannel plate. The reticon diode arrays may be read with a 2 ms frame time for a single spectral line, or a 16 ms frame time in the survey mode. In the X-ray region a curved crystal Johann configured spectrometer observed the Lyman series from 1s-np with n extending towards the series limit. This instrument had a microchannel plate detector with a fast delay-line read-out, histogrammed into a CAMAC resident memory every 3 ms, and was capable of a count rate of over 100 kHz. The crystal and grazing incidence spectrometers directly viewed the A-line. A detailed picture of the spectrometers viewing B-line is shown in Fig 2. The four neutral injectors on DITE are each capable of delivering 600 kW of 25keV hydrogen neutrals in a 100 ms pulse. They cannot be monitored for each shot, and a look-up table of power versus source parameters was used to evaluate the beam powers for each discharge. Other routine measurements available included the central electron density from interferometry, electron temperature from ECE emission and the ion temperature from the energy spectrum of escaping neutrals. Electron density and temperature profiles were only obtained over a series of similar shots. This information is required in the beam attenuation code which calculates the neutral density at the spectrometer viewing position. This leads to errors in the derived impurity density. For the examples of line emission shown in Fig 6 and Fig 7, the plasma had a peak density of approximately 5×10^{13} cm^{-3} and a peak electron temperature of 700 eV. The radial (r) profiles have the forms $n_e(r) = n_e(o) \times 0.9\ (1-(r/a)^2) + 0.1\ n_e(o)$ and $Te(r) = Te,(o)\ (1 - (r/a)^2)^{3/2}$, respectively where the limiter radius is 'a'. The neutral beams were operated between 21kV and 24kV, which gives a typical 1/e attenuation length of 60 cm (for DITE: major radius = 117 cm, minor radius = 26 cm). The DITE injectors have three major components of energy V,V/2,V/3 with the currents in the ratio 48%, 22%, 30% respectively.

3. THEORY

For our ~25keV beam energy the C/X process populates levels indicated by the shaded region in Fig 3. The insert shows a detailed picture of the n=6 shell. The energy levels are calculated from the Dirac equation including only terms to order $(v/c)^2$, which results in

degeneracy with respect to angular quantum number j. In practice higher order relativisitic terms and Quantum Electrodynamical terms lift this degeneracy. The free ion atomic structure is perturbed by the plasma environment which may "mix" some (n,l) levels. Indeed a modified quantum description of the levels can be more appropriate. Some processes to be considered are:

1) Collisions which mix the populations of the nearly degenerate states of the hydrogenic ions. This is more important for higher n-states which have narrower fine structure and longer lifetimes against radiative decay. For given environmental conditions, this gives a critical value for (n,l) above which the relabelled states which differ by $\Delta j=0$ may be considered statistically mixed.

2) The ions are subject to electric fields from their thermal motion ($E=V \times B \sim 1 \times 10^5$ V/M) in the magnetic-fields and from plasma micro-fields ($E \sim 4 \times 10^4$ V/M for $n_e = 5 \times 10^{13}$ cm^{-3}). Stark mixing for states which differ by $\Delta j=0$ can become important for quite low n states. (Omidvar, 1983).

3) Zeeman shifts and other external fields couple $\Delta j=1$ states. (Carolan et al (1984)).

The magnitude of these effects is considered by Isler and Langley (1985). For the DITE plasma we deduce: states which differ by $\Delta j=0$ should be considered mixed for $n > 2$. Stark mixing may be neglected, but for the highest n,l states Zeeman coupling is possible. $\Delta j=0$ mixing is introduced into the strict cascade model by statistically redistributing the population between states of the same J for $n>2$. Following this prescription the recalculated effective emission cross sections differ little from those assuming no $\Delta j=0$ mixing. Although Zeeman coupling occurs for too high an n state to have much effect on the effective emission cross section in DITE, in other experiments with a higher magnetic-field strength, and with increased population into higher n states, which occurs as the neutral beam energy is raised, the cascade will be affected considerably. Strong l selection rules will no longer apply and if the p-state becomes coupled to a state populated directly by C/X, decay directly to the ground state will dominate, and bleed the excited states through the X-ray transitions, (see below).

Recently, there has been considerable interest in experimental measurements(see this conference proceedings) supported by better theoretical calculations of the partial (n,l) cross sections (Green et al (1982), (Shipsey et al (1983)). To calculate the effective

emission cross sections a strict cascade model is first used, with n and l considered strict quantum numbers. The results of this model are shown in Fig 8. Also the extreme case of assuming complete l-state mixing within an n shell is shown for the OVIII ion using the data from Shipsey et al (1983). This is sometimes termed the 'bundled n' model.

Many Ion beam-gas target experiments are now being made (eg: Dijkamp et al) in which the C/X cross sections for an n,l,j state can be derived using a cascade model. It is the purpose of this paper to try to account for the various X-ray and VUV spectral line emissions observed from C/X in a Tokamak plasma. Since for many of the larger machines now being commissioned (JET, TFTR etc.) neutral beams are being used for additional heating, an understanding of the C/X process is essential in order to exploit these beams as a diagnostic of the impurity content.

4. RESULTS AND DISCUSSION

The significant feature of the $\Delta n=1$ VUV transitions is their C/X "signature" ie: their intensities follow the beam current. For the DITE injectors the beam current rise and fall time is less than 1 ms, and the signature is clearly visible, Fig 6. In contrast, the temporal behaviour for the X-ray intensities is more complex and follows changes in the ionisation balance and ion transport resulting from injection. Changes in the electron density and in the absolute abundance of oxygen impurity during injection will also contribute to the line intensity, but these variations are observed to be small. The OVII 1s-1s3p line, Fig 7, shows little evidence of a large change in the oxygen influx during the injection period and the electron density increases at most a factor of two during injection, and typically rather less than this. The reason that the X-ray and VUV emissions from the same principal quantum level are dissimilar must lie in the l-state populations. The Lyman transitions are restricted to radiative decay of the l=1 sub-levels in the ion, whereas the UV transitions have contributions from higher l-levels which are populated by C/X. For transitions involving the higher quantum states studied, n=5 to n=8, where one might predict partial l sub-level smearing (Fonck et al 1984), the C/X cross sections for V(H°) = 25 keV have already fallen by ~ 100, from the peak at n=5 (Janev 1983). It is perhaps for this reason that neither the resonance lines nor the $\Delta n=1$, (for these higher n-state), lines in DITE exhibit the C/X signature.

In order to calculate the contributions to the observed line intensities from C/X recombination of O^{8+} and from electronic

excitation of O^{7+} we first need to estimate the relative abundances of the ions in the plasma. For the O^{8+} concentration we use the $\Delta n=1$ transitions in the VUV and XUV regions which have a clear C/X signature. Using an H° beam attenuation code (Isler et al 1981), the energy component distribution in the beam (Fielding and Stork 1982), and the effective C/X emission cross sections from Fig 8, the following C/X line irradiances have been calculated for 2% Oxygen impurity relative to the appropriate electron density corresponding to the shot.

Transition	Intensity (OVIII)
n = 1 - 2	1.0 GR
n = 2 - 3	0.77 GR
n = 3 - 4	0.28 GR

(1GR = 1×10^{15} ph $cm^{-2}s^{-1}$)

These calculated irradiances correspond to different discharges with somewhat different plasma conditions, and so the relative C/X emissions are not expected to be completely consistent with the relative C/X cross sections. No correction, typically +20%, Isler et al (1981), has been made for the contribution from halo neutrals, ie neutrals resulting from C/X of the H^0 beam with plasma ions. The crystal instrument is further downstream and the increased beam attenuation at this location lowers the C/X irradiance by a further factor of 5-10, depending on the electron density. Using the n = 2-3 and n = 3-4 line intensities (Fig 6) together with an absolute intensity calibration curve for the Grazing Incidence instrument, Fig 4, the impurity density is calculated to be:

$$N(OVIII)/n_e = 0.02\ (-0.01,+02)$$

The calculated N(OVIII) distribution, Fig 9, shows possible variations due to changes in an assumed impurity transport. This distribution can be measured by Abel inversion of the experimental OVIII C/X intensity profile using a series of radially scanned shots. Fig 5 clearly shows the signature of the C/X radiation, but this profile may not be used generally since it corresponds to a particular sequence of similar discharges.

Prior to injection, the OVIII ground state abundance is low and most of the core oxygen ions are completely stripped at $T_e > 500$ eV. Electronic excitation of the Lyman 1-2 line is estimated to give an irradiance of $\sim$ 3-5 GR. At the grazing incidence spectrometer position, this is larger than the calculated Lyman 1-2 signal from C/X, which is still further reduced at the crystal position. The

lack of a C/X signature for the Lyman 1-2 (Fig 6 and Fig 7) transition is thus expected. The lines involving higher quantum levels can be scaled from the observed irradiances, above, by the relative electron impact rates and C/X rates as a function of n,l Fig 8. The reduction in the $\Delta n=1$ C/X cross sections and the increase in the resonance transition should be noted in the case of statistical l sub-level population. Even in the extreme, and unlikely, case of complete statistical population between the l levels the increase in the C/X cross sections for the resonance transitions is not sufficient to compete with that for electron impact excitation at the crystal instrument position. The rate for the latter process may be scaled from the OVIII Lyman 1-2 using published values for hydrogen. The increase in the intensities of the higher members of the Lyman series during beam injection, figure 7(c), can only be due to impact excitation following changes in ionisation balance, since in this particular case the beams are not viewed directly. We thus note that the lack of a clear C/X signature for the Lyman 1-2 through 1-6 is in agreement with our calculations even in the (extremely unlikely) case of complete l state mixing (Sampson (1977)). For our experimental conditions the higher members of the Lyman series are always more easily excited by electron excitation than the C/X process but for the $\Delta n=1$ transitions $1<n<7$, C/X is the dominant process. It is worth noting that even at the grazing incidence observation position the attenuation of the beam is greater than 80%. In principle, by observing the beam closer to its entry point into the plasma, the C/X contribution to the signal could be made to compete with impact excitation even for some of the resonance transitions.

$\Delta n=1$ (visible) transitions between higher quantum states ($n\gtrsim 7$), have been observed to be enhanced during neutral injection in some Tokamaks using higher neutral beam energies (Groebner et al 1984, Suckewer, Skinner et al 1984) but in these cases the situation is less clear. Proton collisions together with motional Stark and Zeeman splitting will smear the populations of some sub-levels and these 'Rydberg atom', $\Delta n=1$ transitions could then be excited either by electron impact from the ground state initially into low l or through C/X initially into sub-levels with $l\sim n$. If impact excitation dominates, even the $\Delta n=1$ transitions will not show the C/X signature, but instead follow changes in the ionisation balance caused directly by the beam injection or by an increase in cross field diffusion, as has been observed to accompany beam injection, Isler et al (1983).

Pengelly and Seaton (1964), have calculated the proton collision rate between l-states in excited hydrogen and their results have been adapted by Fonck et al (1984) to model hydrogenic impurities in Tokamak

plasmas. From their estimates we would expect principal quantum shells for n>6 to start showing partial statistical population for the DITE plasma where ne $\lesssim 5\times10^{13}cm^{-3}$. $\Delta n=1$ transitions involving principal quantum shells well above the maximum for C/X population, (n(max)=5 for oxygen for a beam energy of 25 keV), have been observed in DITE and other tokamaks, but without the C/X signature. The relative cross section for C/X for the different quantum states (Salop 1979, Janev 1984) when normalised to our 1-2, 2-3, 3-4 data indicates that, for our conditions at least, these high quantum transitions which lie in the visible spectral region arise not from direct C/X but more probably from changes in the ionisation balance.

5. CONCLUSION

A clear indication of C/X radiation has been observed on the DITE tokamak, which is consistent with a model dominated by the C/X population process. Using a simple cascade model, and an absolutely calibrated instrument, the oxygen impurity density has been measured. The $\Delta n=1$ "Yrast" transitions show the most clear C/X signature. With a beam energy $\lesssim$ 25keV, these lines all lie to the UV and XUV regions. The model used to calculated the impurity density from the C/X signature does not require the inclusion of other excitation processes.

Other transitions, especially the resonance series and transitions between high Rydberg states n>>6 must be treated with caution and should not be assumed to result solely and directly from C/X even though they are observed only during beam injection. The explanation of these intensities is likely to be very machine specific ie: the intensities will depend on a combination of factors including beam energy and current, viewing position, electron density and temperature, magnetic field, and the density of beam "halo" and background thermal neutrals in the plasma.

REFERENCES

1. P Carolan, M J Forrest, N J Peacock, D L Trotman, (to be published (1985)).

2. W H M Clark J G Cordey, M Cox, S J Fielding, R D Gill, R A Hulse, P C Johnson, J W M Paul, N J Peacock, B A Powell, M F Stamp, D F H Start, Nucl Fusion 22 No 3 333-345 (1982).

3. Dijkamp D, Cirik D, de Heer F J, Vilieg E and Drentje A G, Proc of Int Conf on Physics of Highly Ionised Ions, to be published Nucl Inst Meth (1985).

4. Fielding S J and Stork D, Nuclear Fusion 22 No 5 617 - (1982).

5. R J Fonck, D S Darrow and K P Jaehnig, Phys Rev A29 3288-(1984).

6. R J Fonck, M Finkenthal, R J Goldston, D L Herndon, R A Hulse, R Kaita, D D Meyerhofer, Phys Rev Lett 49 737 - (1982).

7. R J Fonck, R J Goldston, R Kaita and D E Post, Appl Phys Letter 42 239 - (1983).

8. T A Green, E J Shipsey and J C Browne, Phys Rev A25 1364 - (1982).

9. Groebner R J, Burrell K H, et al, Bull APS, 26th Ann Plasma Phys, Meet, Boston, 29 No 8 363 - (1984).

10. Groebner R J, Brooks N H, Burrell K H, Rother L, Appl Phys Letts 43 No 10 920 - (1983).

11. N C Hawkes and N J Peacock, to be submitted to Nucl Fusion (1985).

12. R C Isler, Proc of Int conf on Physics of Highly Ionised Ions to be published Nucl Inst Meth (1985).

13. R C Isler, L E Murray, E C Crume, C E Bush, J L Dunlap, P H Edmonds, S Kasai, E A Lazarus, M Murakami, G H Neilsen, V K Pare, S D Scott, C E Thomas, A J Wootton, Nuclear Fusion 23 No.8, 1017-1037 (1983)

14. R C Isler and L E Murray, App Phys Lett 42 355- (1983).

15. R C Isler, L E Murray, S Kasai, J L Dunlap, S C Bates, P H Edmonds, E A Lazarus, C H Ma, M Murakami, Phys Rev A 24, No5, 2701-2712 (1981).

16. R C Isler and R A Langley, Applied Optics, in press, (1985).

17. R K Janev, Physica Scripta Vol T3 208 - (1983).

18. K Omidvar, Atom Data and Nucl Data tables 28 215-238 (1983).

19. R M Pengelly and M J Seaton, Mon Not R Astro Soc 127 165- (1964).

20. A Salop, J Phys B 12 919 (1979).

21. D H Sampson, J Phys B. 10 749 - (1977).

22. E H Shipsey, T A Green and J C Browne, Phys Rev A 27, 821-, (1983).

23. C H Skinner, S Suckewer, S A Cohen, G Schilling, R Wilson and B Stratton Phys Rev Lett 53 No 5 458 - (1984).

24. S Suckewer, C H Skinner, B Stratton, R Bell, A Cavallo, J Hosea, D Dwang and G Schilling Appl Phys Lett 45 No 3 238 - (1984).

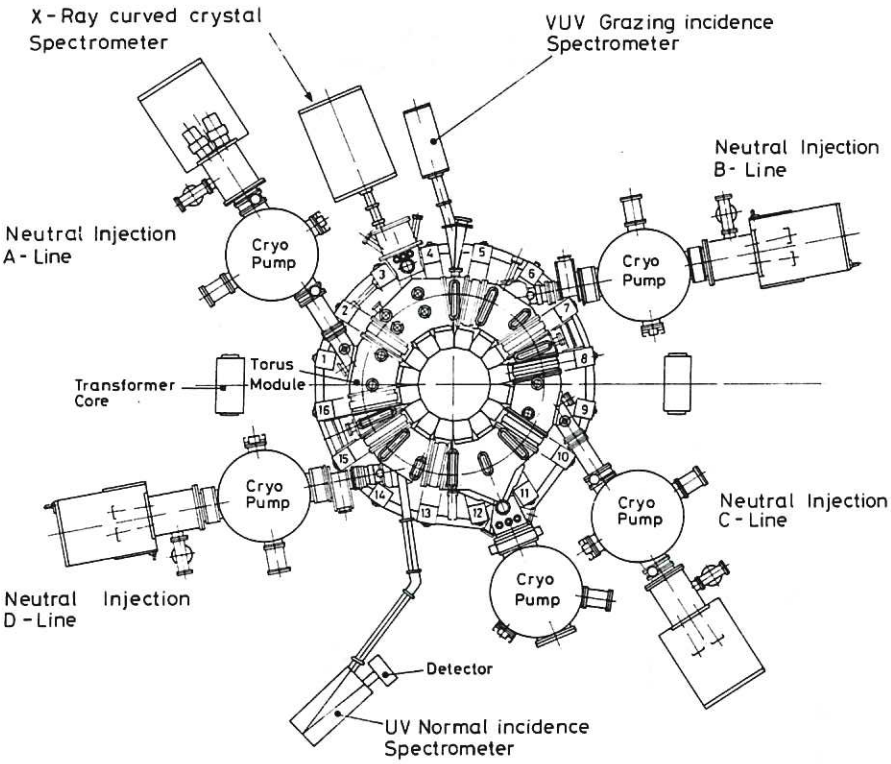

Fig. 1 Plan view of the DITE area. The positions of the three instruments round the machine are indicated. Note that the crystal and grazing incidence instruments view only the B-line, and the normal incidence instrument the A-line.

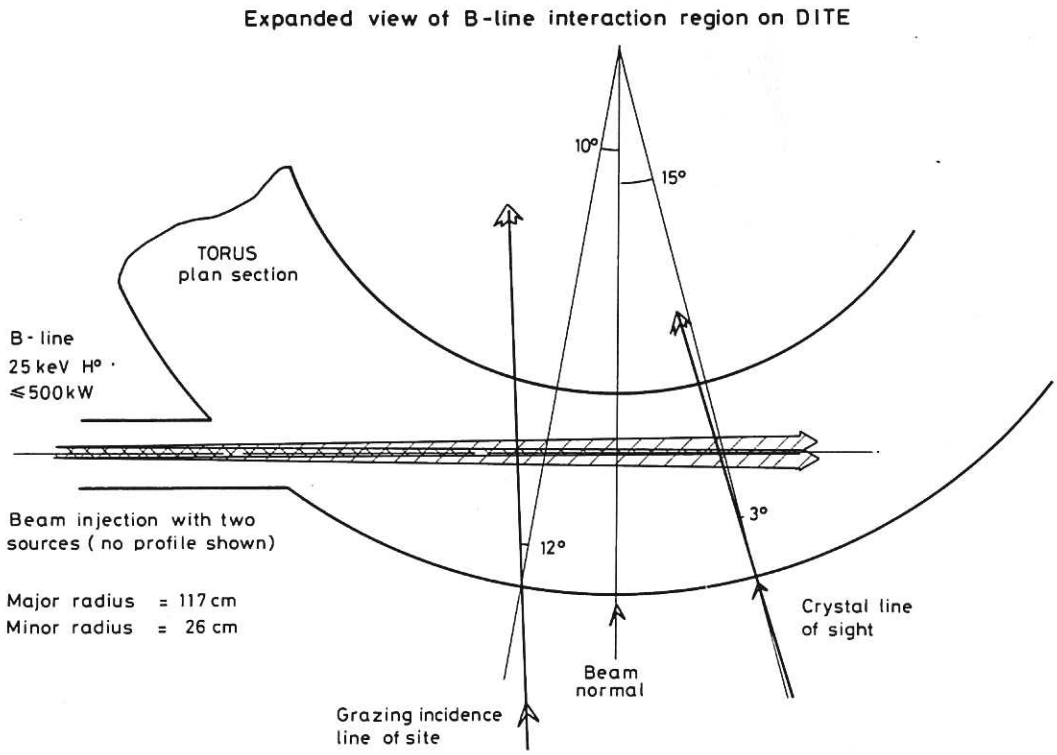

Fig. 2 Detailed view of the beam plasma interaction region for the spectrometers on B-line. These positions and instrument orientations are required to calculate the beam density along the line of sight.

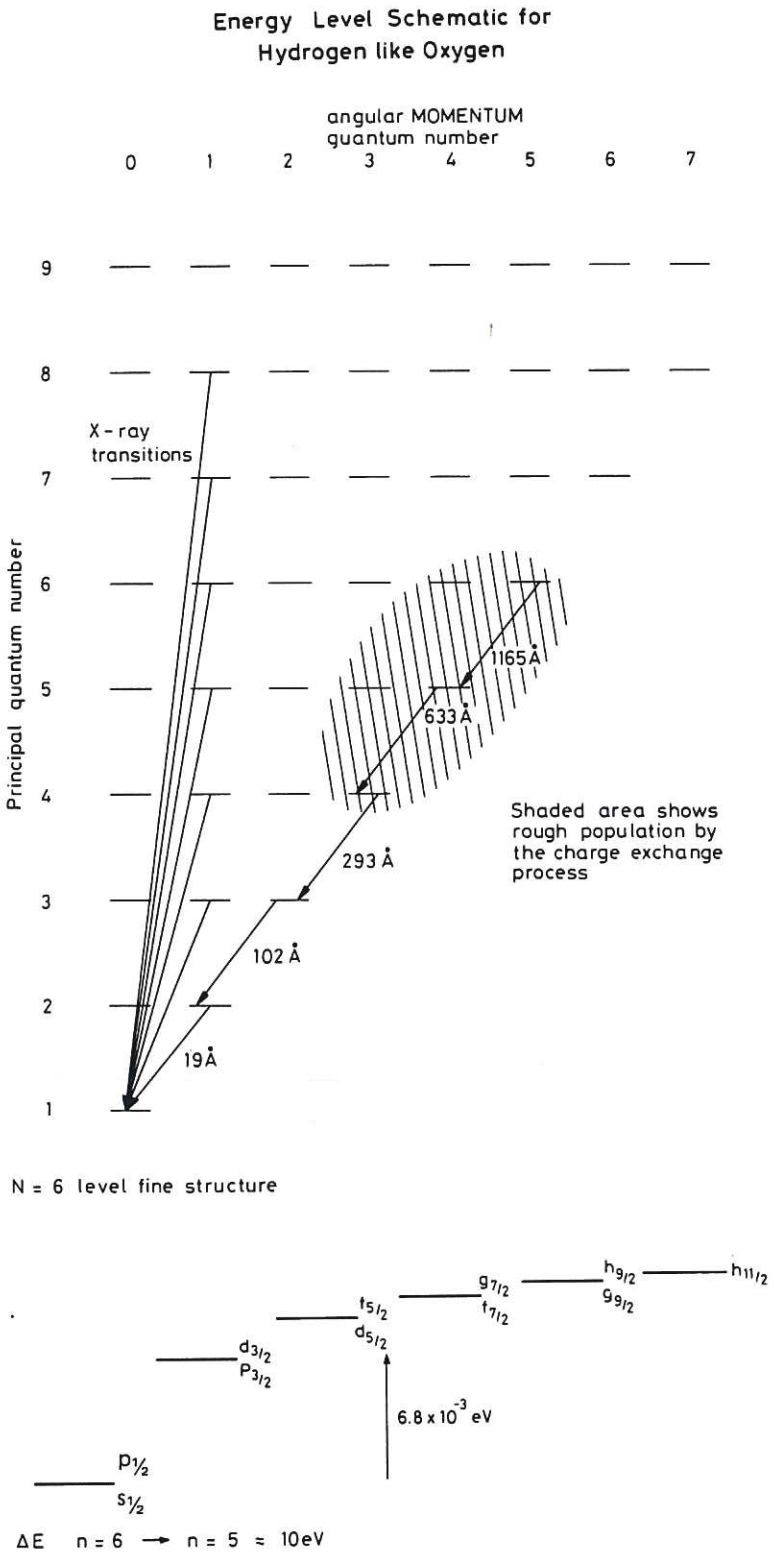

Fig. 3 A schematic of the energy levels for hydrogen-like oxygen. The region populated by the C/X process is indicated, together with the observer transitions. Note the clear decoupling of the Lyman transitions from the $\Delta n = 1$ transitions showing the C/X signature.

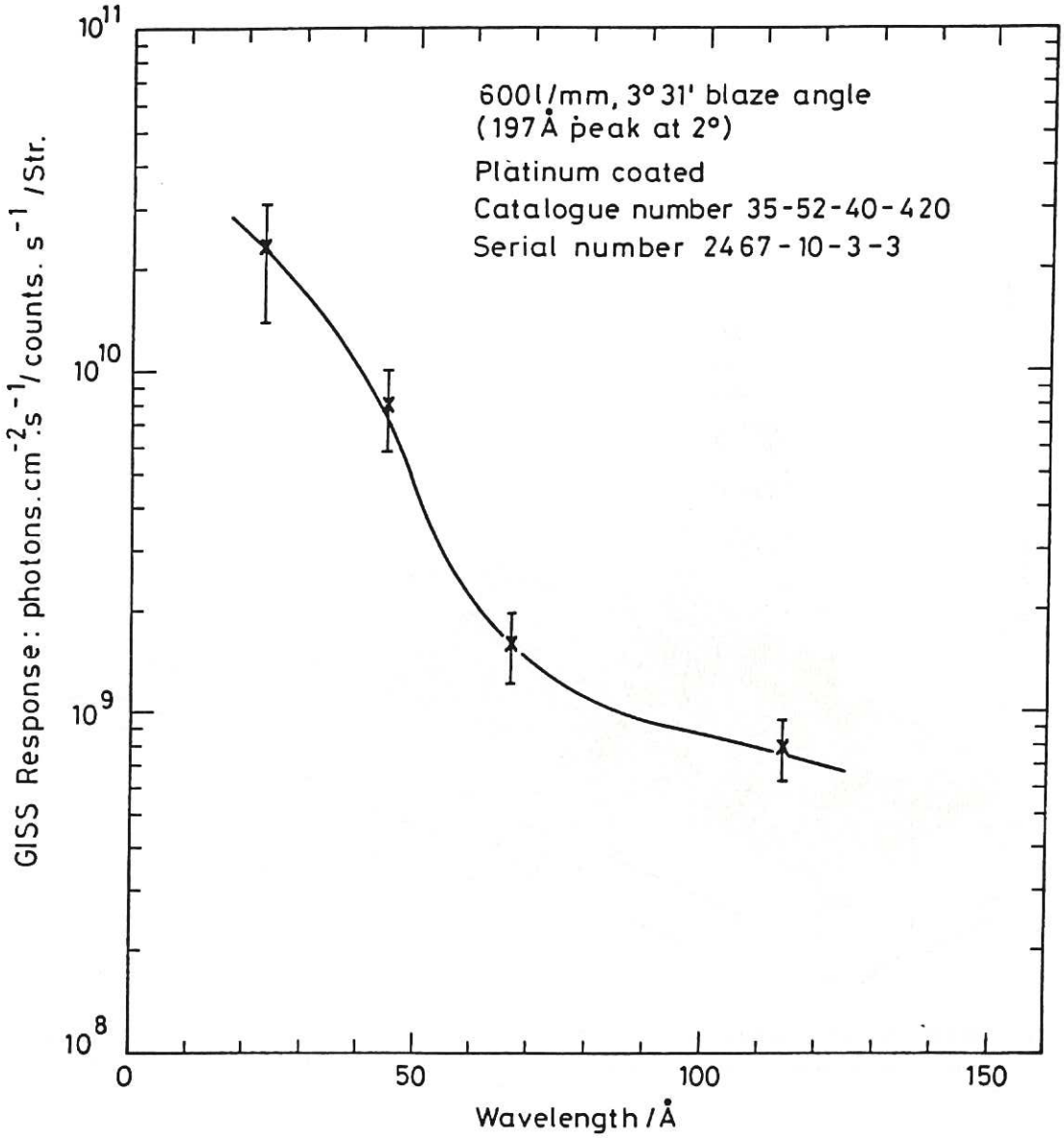

Response of GISS Instrument viewing DITE

Fig. 4 Absolute intensity calibration curve for the grazing incidence instrument. This is used to calculate the impurity density of OVIII.

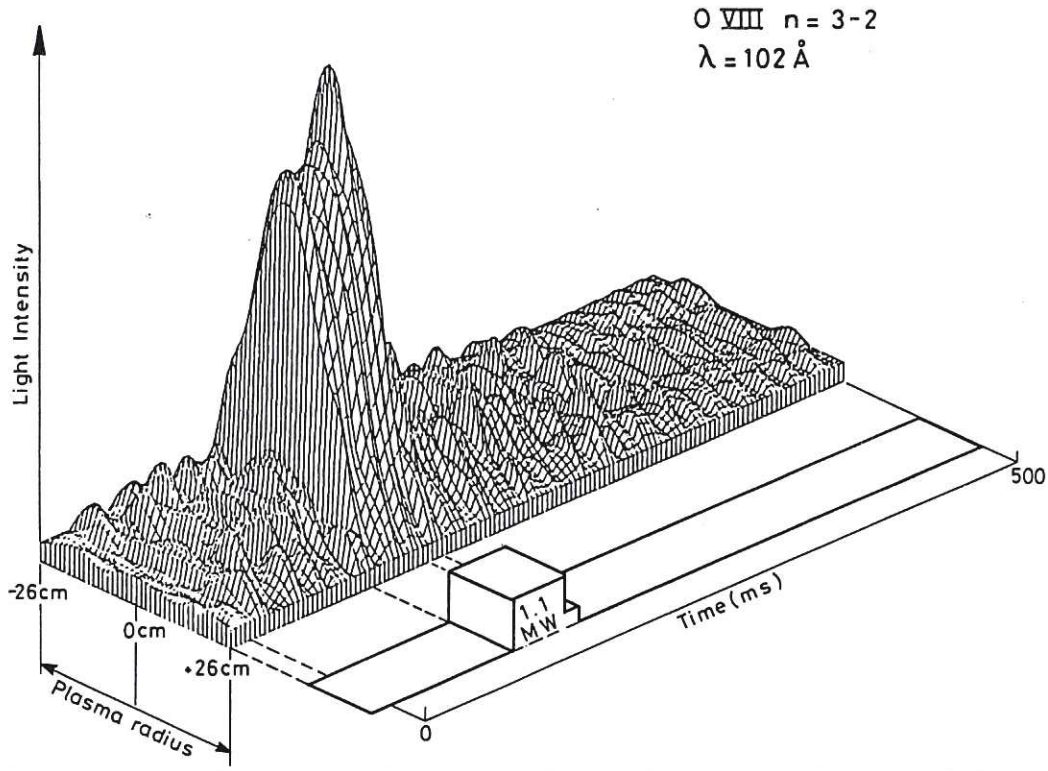

Fig. 5 A measurement of the radial emission profile of OVIII (n = 3 - 2, 102 Å) for an injected shot (a series of radial scans were taken for similar shots and the result Abel inverted). This clearly shows the C/X signature at the start of injection of 100 ms.

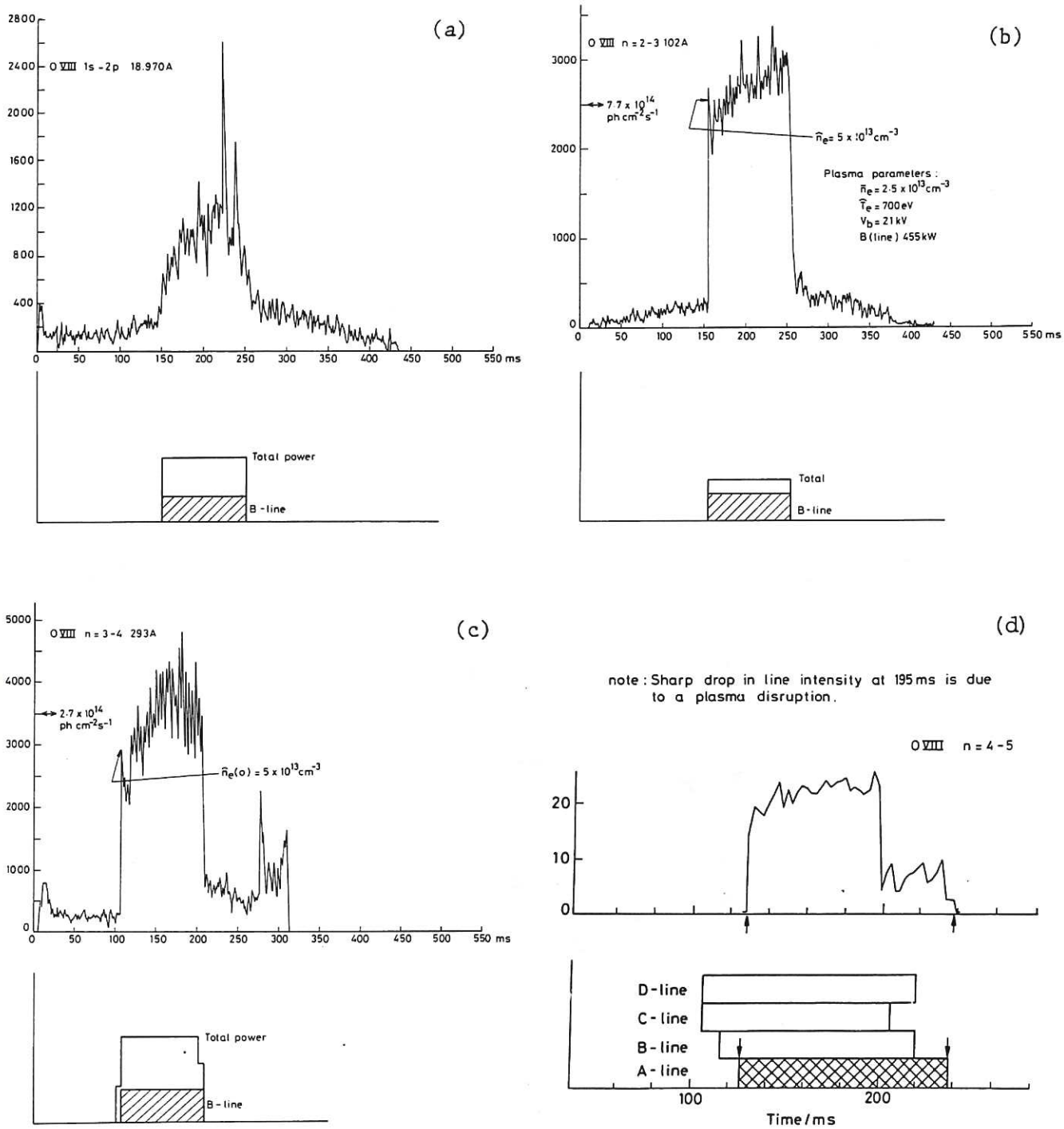

Fig. 6 (a) n = 2 - 1 (b) 3 - 2 (c) n = 4 - 3 transitions in OVIII as observed by the grazing incidence spectrometer. (d) n = 5 - 4 transition as observed with the normal incidence spectrometer. The beam injected power is shown inset on each picture. The hatched regions indicate the beam line viewed by the spectrometer. Note: the C/X signature on (b) and (c) but not on (a) also the sharp drop in intensity at 195 ms (d) is due to a plasma disruption.

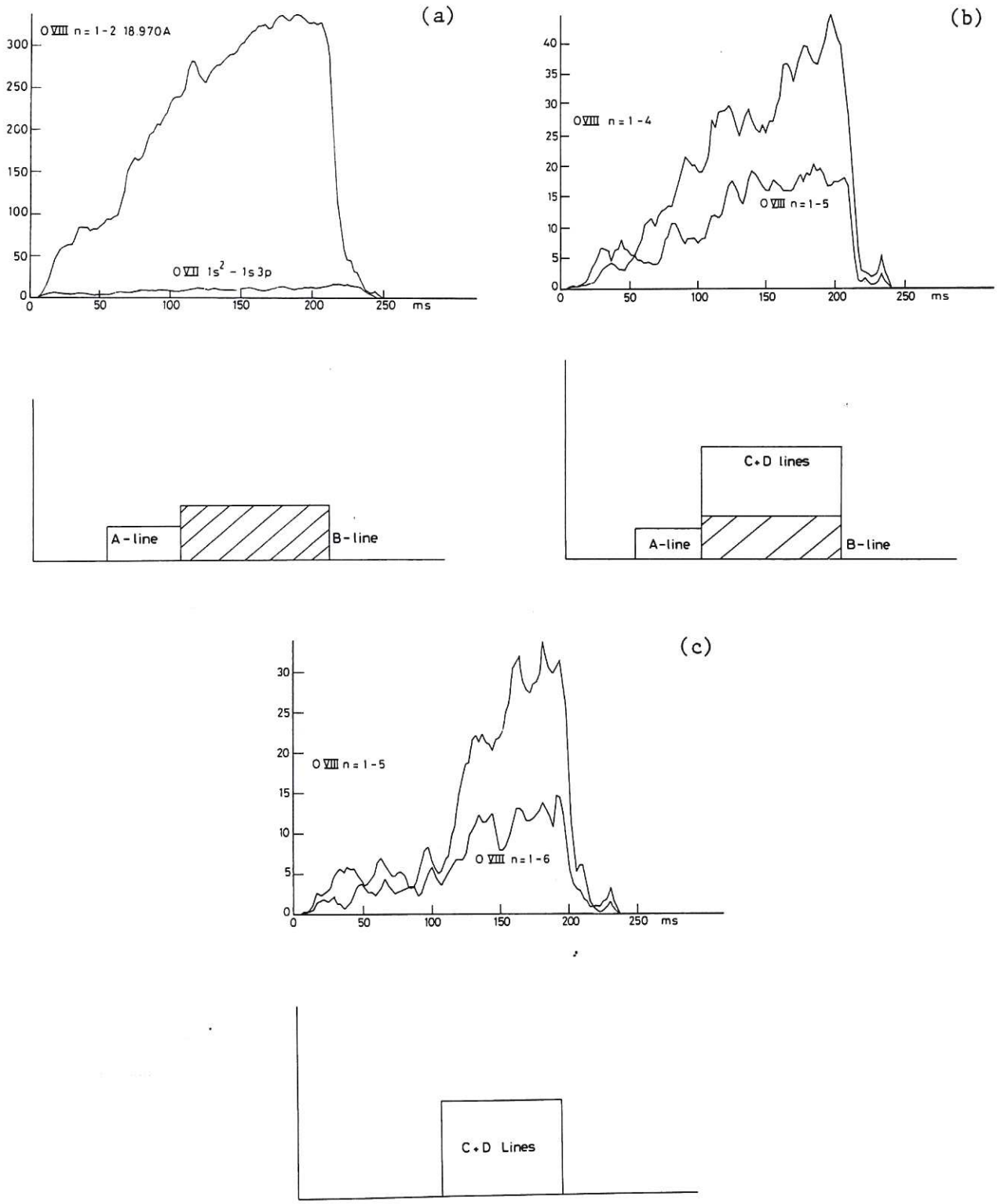

Fig.7 Lyman transitions observed by the crystal instrument. The beam currents are shown inset. The hatched regions indicate the beam line viewed by the spectrometer. The crystal instrument is downstream from the UV spectrometer and the beam attenuation at this location is typically over 95%. (Ordinate in arbitrary units of intensity, Abscissa in ms).

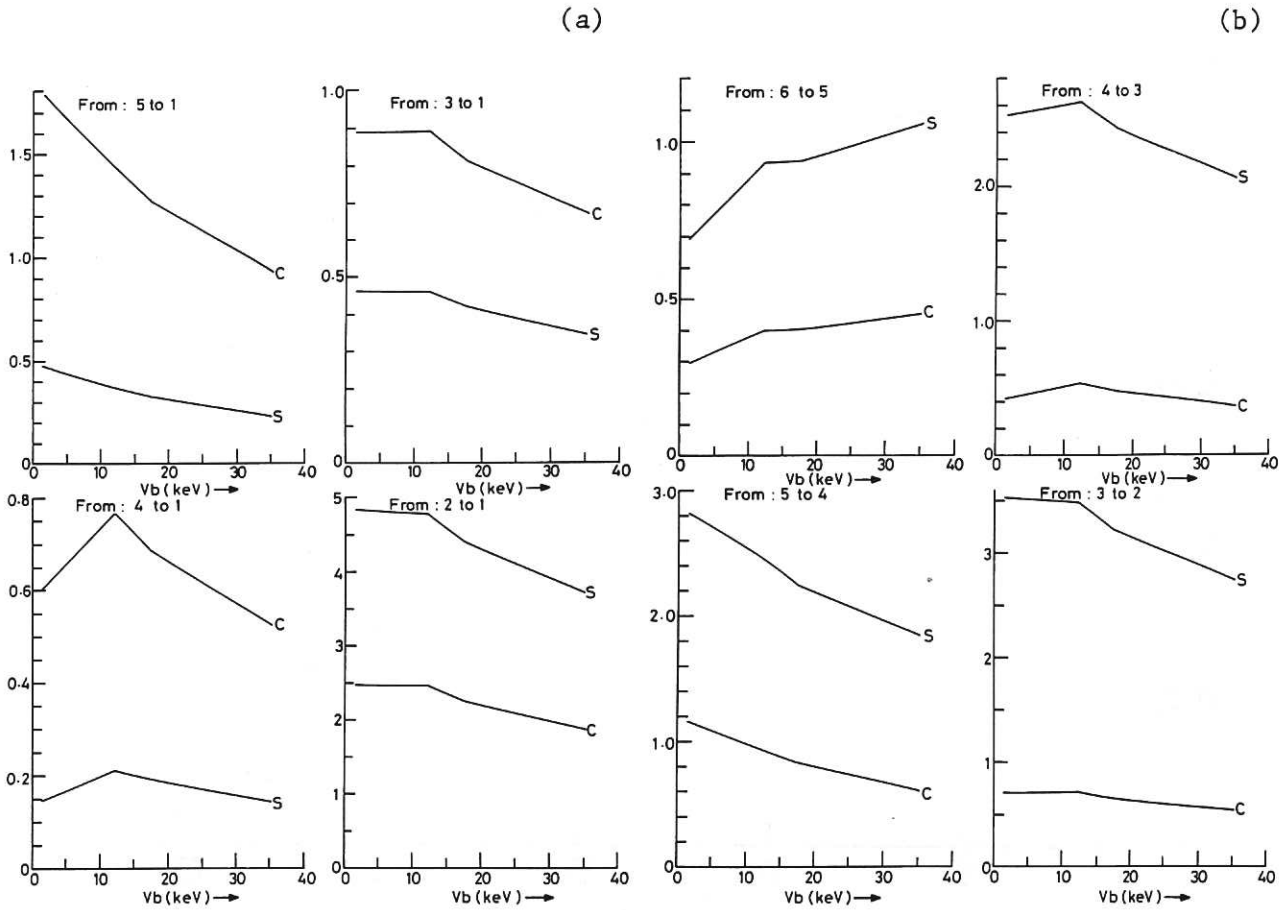

Fig. 8 Cascade model calculations for the effective emission cross section for the indicated transitions in OVIII against neutral energy. Each picture shows two cases: "S" is the result of a strict cascade where n and l quantum numbers selection rules are strictly obeyed. "C" is the result for complete l state mixing in each n-shell. The effect of the Lyman transitions bleeding the $\Delta n = 1$ rate is evident (Shipsey et al (1983) data is used). Cross sections in units of 1×10^{-15} cm^2.

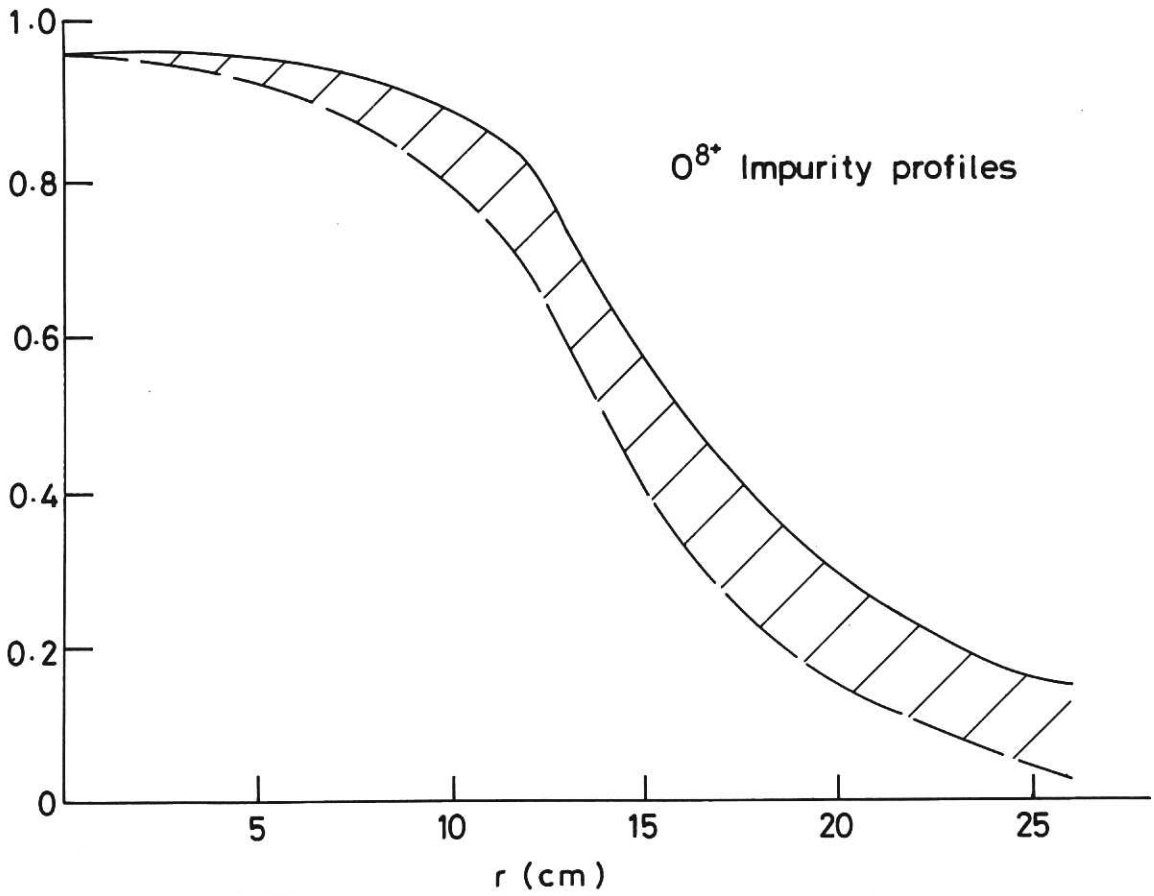

Fig.9 Impurity profiles used in the calculation of the theoretical C/X signal. The shaded area shows the possible uncertainty using different impurity diffusion coefficients.